Carbohydrate Polymers 370 (2025) 124385

Contents lists available at ScienceDirect

Carbohydrate Polymers

journal homepage: www.elsevier.com/locate/carbpol

Structural elucidation and serological studies of emerging *Klebsiella pneumoniae* capsular polysaccharides K102 and K112

Neil Ravenscroft [a], Francesca Nonne [b,1], Gianina Florentina Belciug [b], Michela Zaro [c], Mariagrazia Molfetta [b], Roberta Di Benedetto [b], Renzo Alfini [b], Siwaphiwe Mfana [a], Barbara Bellich [d], Marco Maria D'Andrea [e], Martina Carducci [b], Omar Rossi [b], Carlo Giannelli [b], Paola Cescutti [c], Francesca Micoli [b,*]

[a] Department of Chemistry, University of Cape Town, Cape Town, 7700, South Africa
[b] GSK Vaccines Institute for Global Health, Siena, Italy
[c] Department of Life Sciences, University of Trieste, Via L. Giorgieri 1, Bdg C11, 34127, Trieste, Italy
[d] Institute for Maternal and Child Health - IRCCS "Burlo Garofolo", Trieste, Italy
[e] Department of Biology, University of Rome "Tor Vergata", Rome, Italy

ARTICLE INFO

Keywords:
Klebsiella pneumoniae
Serotype
K-antigen
Structure elucidation
NMR spectroscopy
Vaccine

ABSTRACT

Klebsiella pneumoniae (*Kp*) is a gram-negative bacterium and a leading cause of several severe infections, including neonatal sepsis in low- and middle-income countries (LMICs). *Kp* strains display surface carbohydrates, capsular polysaccharides (CPS) and O-antigens, and are classified by capsule serotyping of the CPS into K-antigens. KL102 and KL112 CPS loci have been identified in two *Kp* high-risk clones, including those associated with neonatal sepsis, being therefore interesting potential targets for vaccine development. Sugar analysis and one- and two-dimensional ^{1}H and ^{13}C NMR spectroscopy studies elucidated the repeating unit structures of the K102(KL102) and K112 (KL112) K-antigens. Interestingly, KL102 is strongly associated with strains of the *Kp* Sequence Type (ST) 307 high-risk clone. Also KL112 was a K-locus which is prominently associated to the major clade of the *Kp* ST15 high-risk clone.

K102 and K112 glycoconjugates were generated and corresponding hyperimmune sera from rabbits showed some levels of cross-binding (by flow cytometry) and cross-functionality (by serum bactericidal activity) against a panel of heterologous K-types isolated from LMICs.

In conclusion, the structures of two new CPS frequently associated with two *Kp* high-risk clones were elucidated and the potential for simplification of vaccine design through cross-reactivity investigated.

1. Introduction

Klebsiella pneumoniae (*Kp*) is one of the most common causes of multidrug resistant (MDR) hospital-acquired infections and the leading etiology of neonatal sepsis globally (Dangor et al., 2024). In 2019, carbapenem and third-generation cephalosporin-resistant *Kp* were estimated to have caused approximately 50,000 deaths each ("Global burden of bacterial antimicrobial resistance in 2019: a systematic analysis", 2022). The rising concern of multidrug resistant infections makes it a public health priority (WHO bacterial priority pathogens list, *2024: Bacterial pathogens of public health importance to guide research, development and strategies to prevent and control antimicrobial resistance*, 2024) to address with alternative solutions to antibiotics. The worldwide spread of MDR *K. pneumoniae* is largely due to the global dissemination of few clonal lineages, called high-risk clones, which accounts for the majority of strains associated with severe infections. This peculiar epidemiological trait provides a strong rationale for the design of multivalent vaccines with wide-spectrum against *Kp*. *Kp* vaccines will target vulnerable children, adolescents and adult populations at risk of *Kp* disease such as those with an anticipated prolonged hospital stay, requiring invasive intensive care management, with risk of surgical site infections, device-associated infections, severe acute malnutrition or immunocompromised. To prevent neonatal sepsis a maternal vaccination strategy has been proposed (Dangor et al., 2024), with placental

* Corresponding author.
E-mail address: francesca.x.micoli@gsk.com (F. Micoli).
[1] Present address: Porto Conte Ricerche, Science and Technology Park of Sardinia, Tramariglio, Alghero, Italy.

https://doi.org/10.1016/j.carbpol.2025.124385
Received 1 July 2025; Received in revised form 8 September 2025; Accepted 9 September 2025
Available online 10 September 2025

transfer of protective antibodies to the fetus thereby protecting young infants in the neonatal period and first few months of life while also reducing antimicrobial usage. Modeling suggests that a *Kp* vaccine targeted at pregnant women could avert approximately 80,000 deaths and 400,000 neonatal sepsis cases, predominantly in sub-Saharan Africa and South Asia (Kumar et al., 2023).

Capsular polysaccharide (CPS), designated as the K-antigen, is a key virulence factor of *Kp* which promotes resistance to phagocytosis by macrophages, neutrophils and monocytes (Gonzalez-Ferrer et al., 2021; Hall, 2013; Mandell, Douglas, and Bennett's Principles and Practice of Infectious Diseases (Eighth Edition), 2015; Opoku-Temeng, Malachowa, Kobayashi, & DeLeo, 2022) . CPSs are characterized by a great diversity, with approximately 80 distinct K-antigen serotypes identified by sero-immuno assays, and several additional ones proposed on the basis of genomic characterization of the K-locus (KL) (Lam, Wick, Judd, Holt, & Wyres, 2022; Stanton, Hetland, Löhr, Holt, & Wyres, 2025; Wyres et al., 2016; Xu, Jiayang, Wenqi, Xiuwen, & Ren, 2024).

In a multi-center study on neonatal sepsis performed in seven LMICs in Africa and Asia, 13 of the top-20 most common CPS loci identified (KL2, KL15, KL23, KL24, KL25, KL39, KL54, KL62, KL64, KL102, KL112, KL117, KL122) were also among the top-20 CPS loci identified in bloodstream infections from adults in Asian countries (Sands et al., 2021; Wyres et al., 2020). KL102 and KL112 are among the most prevalent K-loci in *Kp* isolates causing neonatal sepsis in many recent epidemiological studies conducted in LMICs (Argimón et al., 2021; Nonne et al., 2025; Sands et al., 2021).

Here a combination of sugar analysis and one- and two-dimensional ^{1}H and ^{13}C NMR spectroscopy elucidated the CPS repeating unit structures of K102 and K112. Interestingly, KL102 is strongly associated with strains of the *Kp* sequence Type (ST) 307, that has recently emerged as a high-risk clone. Isolates of ST307, often exhibiting resistance to the major classes of antibiotics, including carbapenems, were first identified in the early 1990s and have spread globally in healthcare settings across the Americas, Australia, Europe and several Asian countries, where they contributed to outbreaks in hospitals (Cejas et al., 2022; Peirano, Chen, Kreiswirth, & Pitout, 2020). In addition, a considerable proportion of ST15 Kp strains circulating at worldwide level have been genotyped as KL112, suggesting that they may express a K112 CPS (Argimón et al., 2021; Feng, Zhang, & Fan, 2023; Rodrigues, Lanza, Peixe, Coque, & Novais, 2023).

CPS specific antisera were generated in rabbits and showed some levels of cross-reactivity against a panel of heterologous K-types isolated from LMICs. This can potentially further simplify vaccine design by reducing the number of serotypes required to achieve the desired coverage.

2. Materials and methods

2.1. Materials and reagents

Sodium Chloride (NaCl, ≥99.5 %, code 1.06404), 1,4-Diazabicyclo [2.2.2]octane (DABCO, ≥99 %, code D27802), 1-Cyano-4-dimethylaminopyridinium tetrafluoroborate (CDAP, ≥97 %, code C2776), Sodium phosphate monobasic (NaH_2PO_4, ≥99 %, code S8282), glycine (≥99 %, code G8898), Fucose (Fuc, ≥97 %, code F8150), Rhamnose (Rha, ≥99 %, code 83650), Mannose (Man, ≥99 %, code 63580), N-Acetylglucosamine (GlcNAc, ≥99 %, code A8625), Glucose (Glc, ≥99.5 %, code G7528), Galactose (Gal, ≥99 %, code G6404), Galacturonic acid (GalA, ≥97 %, code 48280), Glucuronic acid (GlcA, 97.5–102.5 %, code G8645), 3 M HCl in methanol (code 90964-10X1mL), Sodium borodeuteride ($NaBD_4$, 98 atom % D, code 205591), Anhydrous pyridine (99.8 %, code 270970), Acetyl chloride (≥ 98.0 %, code 8.22252), Deuterium oxide (D_2O, 99.9 %, code 151882) were purchased from Sigma-Aldrich, USA.

Trifluoroacetic acid (TFA, ≥99 %, code 299537) was purchased from Honeywell, USA. Sodium Hydroxide 50 % solution (NaOH, code 3727) was purchased from JT Baker, USA. Acetonitrile (ACN, ≥99.9 %, code 20060) was purchased from VWR, USA. Sodium acetate (≥99.9 %, code 59326) was purchased from Thermo, USA. Silyl-2110 (HMDS/TMCS/pyridine (2/1/10, code 701480.201) was purchased from Macherey-Nagel Germany. Acetic anhydride (97+ %, code 036292.K3) and Potassium Hydride, (30–35 % *w*/w in mineral oil, code L13266) were from Thermo Fisher Scientific, USA. (*S*)-(+)-2-butanol (98.0+ %, code B09251ML) was from TCI America™, Fisher Scientific USA and Anhydrous DMSO (max. 0.005 % H_2O, ≥ 99.8 %, code 83673.230) was purchased from VWR chemicals, Avantor, USA. CRM_{197} was supplied by GSK, UK.

2.2. CPS isolation and purification

CPS were isolated and purified from bacteria as previously described (Nonne et al., 2024). Kp strains were cultured on Worfel-Ferguson Agar plates (containing yeast extract 2 g/L, $MgSO_4{\cdot}7H_2O$ 0.25 g/L, K_2SO_4 1 g/L, NaCl 2 g/L, and sucrose 20 g/L) and incubated overnight at 30 °C. Following incubation, bacterial biomass was harvested in water (approximately 3 mL per plate). The suspension was then heated at 100 °C for 6 h in a preheated thermoblock heater. Afterwards, the mixture was centrifuged at 4000 rpm for 30 min at 4 °C, and the supernatant containing polysaccharides was collected and filtered using 0.22 μm membranes.

The bacterial supernatant was first lyophilized and then reconstituted in water. The solution was adjusted to a final composition of 240 mM NaCl, 5 mM Na_2SO_4, and 1 % CTAB by adding appropriate volumes of 1 M NaCl, 100 mM Na_2SO_4, and 10 % CTAB. The mixture was heated at 100 °C for 4 h. After cooling at 4 °C for 10 min, the solution was centrifuged at room temperature at 4000 rcf for 15 min. The supernatant was separated from the pellet, diluted 1:10 with 5 mM Na2SO4, and incubated at 37 °C for 1 h. A subsequent centrifugation (15 min, 4000 rcf, room temperature) yielded a pellet containing K-Ag, which was solubilized in 1 M $CaCl_2$. Ethanol (98 %) was added to the solution to achieve a final concentration of 25 % (*v*/v). After incubation for 30 min at room temperature, the supernatant was recovered via centrifugation (15 min, 4000 rcf, room temperature) and further diluted with 98 % ethanol to reach a final concentration of 80 % (v/v). Following a 1 h incubation at room temperature, the pellet containing K-Ag was collected by centrifugation (15 min, 4000 rcf, room temperature) and solubilized in 1 M NaCl. The solution was then purified using an Amicon 10 K ultra centrifugal filter unit (Millipore, Burlington, MA, USA) and subsequently filtered through 0.22 μm Millipore filters (Millipore, Burlington, MA, USA). The process was characterized by overall yields close to 40%.

2.3. Glycoconjugates preparation

K102 and K112 were firstly sonicated (Sonics Vibra cell, Bio Class, Pistoia, Italy) at 130 W for a total application of 30 min in ice bath (with 30 s ON and 30 s OFF cycles), lyophilized and subsequently conjugated to CRM_{197} via CDAP chemistry following the protocol reported by Nappini et al. (Nappini et al., 2024). Briefly, the CPS resuspended in water were activated at the concentration of 1.8 mg/mL PS, in 50 mM DABCO at pH 9, with a CDAP/PS of 1 *w*/w. The reactions were kept in ice bath for 15 min. Then, CRM_{197} in 5 mM DABCO pH 9, 9 g/L NaCl at 19.7 mg/mL was added with a CPS/CRM_{197} weight ratio of 1:1. The reaction mixtures were kept under mixing at 25 °C for 2 h. After conjugation, 1 M glycine in 50 mM sodium phosphate at pH 7 was added in equal volume with respect to the reaction mixtures to quench eventual residual cyanoester groups, and the reaction mixtures were kept at 2–8 °C overnight.

The conjugates were purified using Amicon 100 kDa (Merck, USA) centrifugation devices against PBS (3× 30 min at 1000 rpm, 20 °C). A second ultrafiltration was done using Amicon 30 kDa (Merck, USA) centrifugation devices against PBS (3× 10 min at 3500 rpm, 20 °C).

The purified conjugates were characterized by micro BCA (Thermo Scientific, Waltham, MA, USA) and phenol-sulfuric assay for total protein and total saccharide content, respectively and the CPS to protein ratio was calculated. Conjugates formation was verified by HPLC-SEC, comparing the conjugates with unconjugated CRM_{197} and CPS.

2.4. Glycoconjugates formulation and animal study

"GSK is committed to the Replacement, Reduction and Refinement of animal studies (3Rs). Non-animal models and alternative technologies are part of our strategy and employed where possible. When animals are required, application of robust study design principles and peer review minimises animal use, reduces harm and improves benefit in studies".

Animal sera used in this study were derived from rabbit immunization experiment performed at the Charles River Laboratories (France). The animal studies were reviewed by the local ethical committee (Project code: 2016061011167092 from 11 September 2018 (rabbits)) and carried out in compliance with animal welfare standards according to European Directive 63/2010 and local legislation.

Two female (>1.5 kg) New Zealand White rabbits per group were injected intramuscularly with 500 μL/dose of 25 μg of Kp CPS at days 0 and 28. Formulations were prepared by diluting the CPS-CRM_{197} glycoconjugates in NaCl 9 g/L and Alhydrogel (final Al^{3+} concentration: 0.75 mg/mL). Blood was taken on day 42 (post II) as individual sera and stored at −20 °C.

2.5. Analytical methods

Polysaccharide concentration and sugar composition was determined by HPAEC-PAD as described later. Protein concentration was measured by micro BCA, using bovine serum albumin (BSA) as a reference following the manufacturer's instructions (Thermo Scientific, USA). DNA content was estimated by measuring UV absorbance at a wavelength of 260 nm with Lambda 25 spectrophotometer (Perkin Elmer), assuming that a nucleic acid concentration of 50 mg/mL produces an $OD_{260} = 1$.

2.5.1. High performance liquid chromatography–size exclusion chromatography (HPLC–SEC)

Molecular size distribution of all purified CPS was measured by HPLC-SEC TSK gel 6000PW (30 cm × 7.5 mm) column connected in series with TSK gel 3000 PW_{XL} column (30 cm × 7.8 mm) and a TSK gel PW_{XL} guard column (4.0 cm × 6.0 mm). Pullulans were used to build standard calibration curve (2000–50 kDa range) and. 0.1 M NaCl, 0.1 M NaH_2PO_4, 5 % ACN, pH 7.2 buffer was used as mobile phase at the flow rate of 1 mL/min. Analysis was performed with Acquity UPLC H-Class Bio System (Waters, USA) Polysaccharides peaks were detected by differential refractive index (dRI). UV detection at 260 and 280 nm was used to check absence of nucleic acid and protein impurities. Additionally, fluorescence emission was detected at ex280/em336 nm to check for protein impurities.

2.5.2. High performance anion exchange chromatography with pulsed amperometric detection (HPAEC-PAD)

All samples, diluted to final volume of 450 μL, to have each sugar monomer in the range 0.5–10 μg/mL, were hydrolyzed in 2 M trifluoroacetic acid (TFA) by using a Microwave Reaction System (Anton Paar) with a irradiation power of 700 W (corresponding to 120 °C) for 30 min. The heating time to reach target temperature was set to 10 min for all runs, cooling after the experiment was performed down to 55 °C in 5 min. After the hydrolysis, samples were dried by Speedvac (SPD140DDA-230, Thermofisher, USA), reconstituted in 450 μL of water and filtered using 0.45-um 96-wells plate filters for chromatographic analysis. HPAEC–PAD was performed with a ICS5000 (Thermo, USA) equipped with a CarboPac PA1 column (2 × 250 mm, Thermo, USA) coupled with a PA1 guard column (2 × 50 mm, Thermo, USA). Separation of the monosaccharides was performed with a flow rate of 0.375 mL/min, eluting in 18 mM NaOH over 15 min. Next, a 17 min gradient from 0 to 300 mM of sodium acetate in 150 mM NaOH was eluted. Finally, the column was re-equilibrated with 18 mM NaOH for 20 min. The effluent was monitored using an electrochemical detector in the pulse amperometric mode with a gold working electrode and an Ag/AgCl reference electrode. The resulting chromatographic data were processed using Chromeleon software 7.2 (Thermo, USA). Calibration curves were built with a sugar monomers mixture (Fuc, Rha, Man, GlcNAc, Glc, Gal, Man, GalA, GlcA), each in the range 0.5–10 μg/mL. The standard was treated in the same way as the samples.

2.5.3. Sugar composition and linkage analysis by GLC and GLC-MS

Composition analysis was carried out after methanolysis of the polysaccharide with 3 M HCl in methanol at 85 °C for 16 h followed by derivatization to trimethylsilyl methyl glycosides (TMS) using the Silylating mixture HMDS/TMCS/pyridine (2/1/10) at 80 °C for 30 min (Kakehi & Honda, 2021). To determine the position of the glycosidic linkages, the polysaccharide was permethylated following the protocol developed by Harris et al. (Harris, Henry, Blakeney, & Stone, 1984). Briefly, the polysaccharides were permethylated at room temperature with freshly prepared potassium dimsyl, hydrolyzed with 2 M TFA for 1 h at 125 °C, reduced with sodium borodeuteride ($NaBD_4$) for 16 h at room temperature, and peracetylated with acetic anhydride and pyridine at 100 °C for 30 min (Albersheim, Nevins, English, & Karr, 1967) to give a mixture of partially methylated alditol acetates. For the absolute configuration analysis, samples were converted to trimethylsilylated (+)-2-butyl glycosides (Gerwig, Kamerling, & Vliegenthart, 1979; Gerwig, Kamerling, & Vliegenthart, 1978). The polysaccharides were reacted with 3 M HCl in methanol at 85 °C for 16 h, followed by incubation with (*S*)-(+)-2-butanol and acetyl chloride (12.3:1 = V:V) at 80 °C for 16 h. The obtained butyl-glycosides were derivatized to TMS using the Silylating mixture HMDS/TMCS/pyridine (2/1/10) at room temperature for 1 h. Temperature controlled reactions were performed in a Reacti-Therm I (#TS-18821, Thermo Fisher Scientific, Italy).

The derivatized samples were analyzed by GLC using an Agilent Technologies 6850 gas chromatograph equipped with a flame ionization detector, using He as the carrier gas and a Zebron ZB-5 MSi capillary column (Phenomenex, 30 m × 250 μm × 0.25 μm). The following temperature programs were used: for trimethylsilyl methyl glycosides, 1 min at 150 °C, 150–280 °C at 3 °C/min, 2 min at 280 °C; for partially methylated alditol acetates, 1 min at 90 °C, 90–140 °C at 25 °C/min, 140–200 °C at 5 °C/min, 200–280 °C at 10 °C/min, 10 min at 280 °C; for trimethylsilylated (+)-2-butyl glycosides, 1 min at 50 °C, 50–150 °C at 50 °C/min, 1 min at 150 °C, 150–200 °C at 2 °C/min. GLC-MS analyses were carried out on an Agilent Technologies 7890 A gas chromatograph coupled to an Agilent Technologies 5975C VL MSD using the same column and the temperature programs of the GLC analyses. Values of the integrated area of the partially methylated alditol acetates were corrected by the effective carbon response factors (Sweet, Shapiro, & Albersheim, 1975).

2.5.4. NMR analysis

The molecular size of all purified K-Ags were reduced by using Sonics Vibra cell (Bio Class) instrument for 30 min at 130 W. After confirmation of size reduction by HPLC-SEC, the sample was lyophilized before submission for NMR analysis. Polysaccharide samples (2–10 mg) were dissolved in D_2O and subjected to two cycles of D_2O exchange before transfer to a 5 mm tube (Bruker). Spectra were recorded on a Bruker Avance III 600 MHz NMR spectrometer equipped with a BBO Prodigy cryoprobe and processed using standard Bruker software (Topspin 3.2). The probe temperature was set at 318 K for K102 and 333 K for K112. 1D (^1H and ^{13}C) and 2D, COSY, TOCSY, NOESY, HSQC and HMBC NMR experiments were performed. 2D COSY and NOESY experiments were recorded with pre-saturation of HOD, whereas the TOCSY experiments were performed using DOSY to remove signals from low molecular

weight components (ledbpgpml2s2d). 2D TOCSY experiments were recorded using a mixing time of 150 ms and the 1D variants using 180–200 ms. 2D NOESY experiments and the 1D variants were recorded using a mixing time of 300 ms. The HSQC experiment was optimized for $J = 145$ Hz (for directly attached $^{1}H—^{13}C$ correlations), and the HMBC experiments optimized for a coupling constant of 6 Hz (for long-range $^{1}H—^{13}C$ correlations). To improve sensitivity by performing many scans, the 2D experiments were recorded using non-uniform sampling: 40 % for homonuclear and 20–30 % for heteronuclear experiments. Chemical shifts are expressed in ppm using acetone as internal reference (2.225 ppm for ^{1}H and 31.07 ppm for ^{13}C). The ^{13}C glycosylation shifts reported in **Tables S2** and **S4** were calculated using the chemical shift data reported for the corresponding unsubstituted monosaccharide (Lundborg & Widmalm, 2011).

2.5.5. Sera binding to bacteria by flow cytometry

Klebsiella pneumoniae cultures, grown for 24 h at 37 °C in M63C medium (Nonne et al., 2024), were harvested by centrifugation and washed twice in PBS. Bacterial pellets were incubated with rabbit sera diluted 1:500 for 1 h at RT. Following PBS washes, bacteria were incubated with Goat anti-Rabbit IgG Secondary Antibody, Alexa Fluor™ 488, (Invitrogen) diluted 1:1000 for 30 min at RT. Finally, bacteria were fixed in 4 % formaldehyde (BD Cytofix, Bioscience, USA) for 30 min at 4 °C and resuspended in PBS. All washing steps and antibodies dilutions were performed using 1 % (*w/v*) BSA in PBS. Each strain was also incubated with the Secondary Antibody only, as negative control. We considered positive by FC those samples for which MFI increase respect to negative control was >4. For determination of bacteria binding with anti-CPS antibodies a flow cytometer (BD Accuri C6 Plus Cytometer, BD Biosciences, San Jose, CA) equipped with a blue laser exciting at a wavelength of 488 nm was used. Before each experiment, the calibration of the flow cytometer was assessed with calibration beads (BDTM CS&T RUO Beads; BD Biosciences). Data acquisition was set at 10,000 events per sample, a flow rate of 66 µL/min and a threshold at 5000 on FSC-Height signal. Data was collected using C6 Plus software, analyzed using FlowJo software (FlowJo, Ashland, Oregon) and reported as mean fluorescence intensity (Geometric Mean (FL1-A: FITC-A)).

2.5.6. Serum bactericidal activity (SBA)

SBA conditions were established for one isolate for each K-type, starting from complement sensitivity tests. The same % of Baby Rabbit Complement, identified as the highest % not causing any aspecific killing was then used for all strains sharing same K type (50 % for KL112, 30 % for K 34, K39, KL102, KL105, 25 % for K15, K18, 20 % for K25, respectively).

Rabbit sera were heat inactivated (56 °C for 30 min) and tested against different *Kp* isolates in SBA based on luminescent readout adapting a method previously described (Necchi, Saul, & Rondini, 2017; Rossi et al., 2020). Briefly, different dilutions of test sera were incubated with bacteria in 96-well round bottom sterile plates (Corning, Glendale, AZ, USA) - the SBA plate- in the presence of Baby Rabbit Complement. The HI sera were serially diluted in LB in the SBA plate (25 µL/well) starting from 1:20 dilution (final dilution) followed by 3-fold dilution steps up to 7 dilution points plus one control well with no sera, which represented control for non-specific complement killing as well as a sample diluted infinite-fold. Log-phase cultures for the assay were prepared as follows: frozen −80 °C bacterial working aliquots in 20 % glycerol stocks were grown overnight (16–18 h) at 37 °C in M63 medium (Nonne et al., 2024), stirring at 180 rpm and then diluted in fresh LB medium in order to have an optical density at 600 nm (OD600) of 0.05 and incubated at 37 °C with 180 rpm agitation in an orbital shake, until reaching OD600 of 0.22 ± 0.03 and afterwards diluted to approximately 1×10^{6} Colony Forming Unit/mL in LB. An adequate volume of reaction mixture containing the target bacterial cells (10 µL/well) and Baby Rabbit Complement as an external source of complement in LB was prepared; 75 µL/well of the reaction mixture were added to each well of the SBA plate containing HI serum dilutions (final reaction volume 100 µL), mixed and incubated for 3 h at 37 °C. At the end of the incubation, the SBA plate was centrifuged at room temperature for 10 min at 4000 ×g. The supernatant was discarded to remove ATP derived from dead bacteria and SBA reagents. The remaining bacterial pellets were resuspended in PBS, transferred to a white 96-well plate (Greiner Bio-One, Roma, Italy) and mixed 1:1 v:v with BacTiter-Glo Reagent (Promega, Southampton, UK). The reaction was incubated for 5 min at room temperature on an orbital shaker at 600 rpm, and the luminescence signal was measured by a luminometer (Synergy HT, Biotek, Swindon, UK). A negative preimmune control was added on each plate as well as a hyperimmune serum containing antibodies against an unrelated KAg and no killing was verified.

In L-SBA the level of luminescence detected is directly proportional to the number of living bacteria present in the wells, which is inversely proportional to the level of functional antibodies present in the serum. A 4-parameter non-linear regression was applied to the raw luminescence (no normalization of data was applied) obtained for all the sera dilutions tested for each serum; an arbitrary serum dilution of 10^{15} was assigned to the well containing no sera. Fitting was performed by weighting the data for the inverse of luminescence. To validate the dilution series, the highest luminescence detected in the dilution series at T180 had to be at least 0.7-fold the luminescence detected in the control well with no sera added. Results of the assay were expressed as the IC50, the reciprocal serum dilution that resulted in a 50 % reduction of luminescence and thus corresponding to 50 % growth inhibition of the bacteria present in the assay. GraphPad Prism software (GraphPad Software, La Jolla, CA, USA) was used for curve fitting and IC50 determination. A titer equal to half of the first dilution of sera tested (10) was assigned to not bactericidal sera.

3. Results

3.1. Structural determination of K102 CPS

A panel of *Kp* isolates obtained from Rwanda and Bangladesh and identified as potential new serotype K102 was selected from the BARNARDS study (**Table S1**) (Nonne et al., 2025). The CPS was extracted from all isolates and its amount and saccharide length were determined through a high-level chemical characterization (**Table S1**). Sugar amount varied from 12 to 23.4 µg/OD and molecular weight (MW) from 300 to 436 kDa. All CPS shared the same sugar composition as determined by HPAEC-PAD. The ST307 12641B strain from Rwanda was selected as representative of KL102 and used for in depth structural analysis.

The CPS was purified from 12641B as previously described, after boiling bacteria grown on plates in water (Nonne et al., 2024), through a CTAB fractional precipitation-based process, and resulted in CPS with <2 % protein and < 1 % DNA impurities. It showed an average MW of 360 kDa which was reduced to 160 KDa after sonication. HPAEC-PAD analysis indicated the presence of Gal, Glc, and GlcA. Composition analysis using methanolysis followed by trimethylsilylation derivatisation and gas liquid chromatography-mass spectrometry (GLC-MS) analysis confirmed the presence of Gal, Glc and GlcA in the molar ratio of 3.0:2.0:0.7, indicating the presence of a hexasaccharide RU. Linkage analysis of the neutral monosaccharides, performed by GLC-MS analysis of the partially methylated alditol acetates identified: terminal Glc*p*, 3-Gal*p*, 6-Gal*p*, and 3,4,6-Gal*p* in the molar ratio of 2.17:1.17:1.00:0.35. GlcA was determined to be in the side chain by NMR analysis. The D absolute configuration was established for all sugar residues.

Detailed 1D and 2D ^{1}H and ^{13}C NMR experiments were performed. 1D proton NMR and DOSY spectra (Fig. 1) showed that the KL102 spectrum contained six anomeric signals (designated A to F) at 5.45, 5.06, 4.81, 4.67, 4.65, and 4.50 ppm, consistent with serotype K102 possessing a hexasaccharide RU with two α- and four β-monosaccharides.

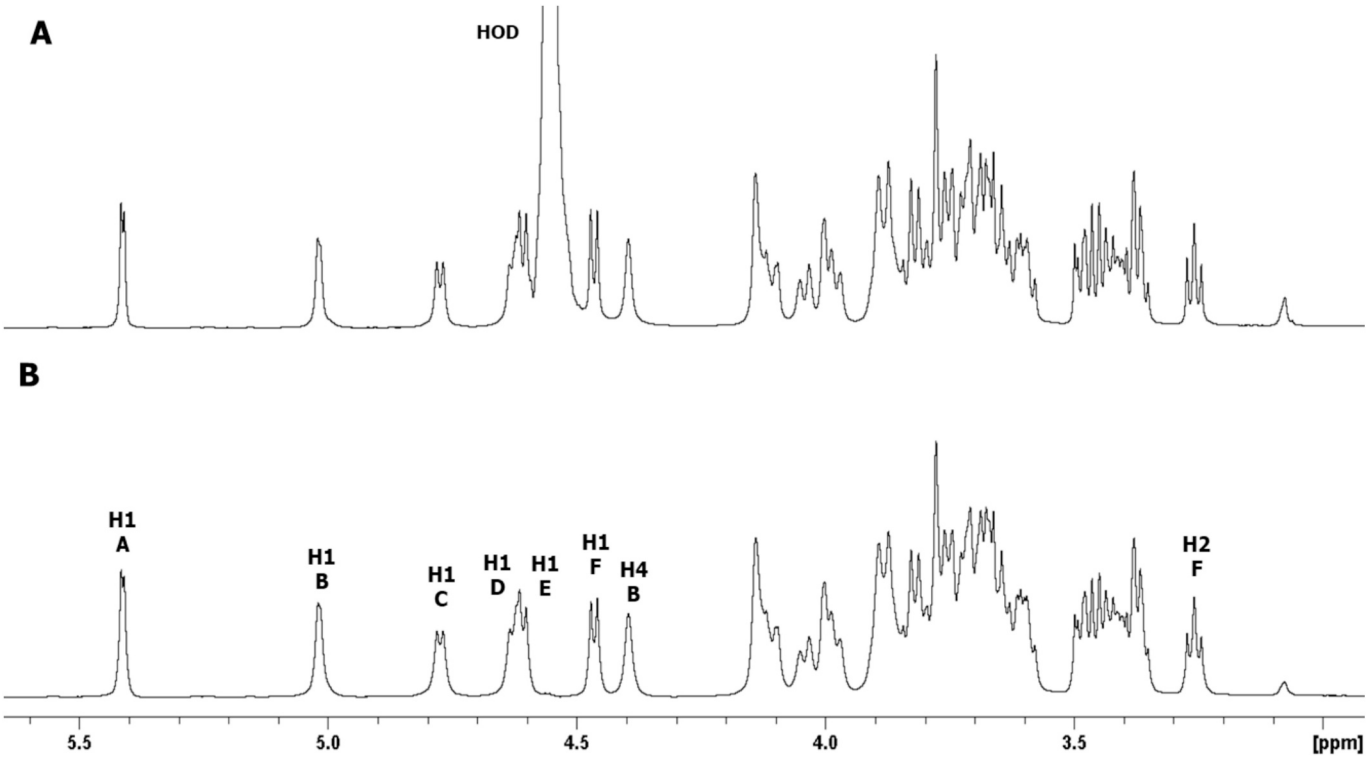

Fig. 1. ^{1}H NMR spectra of KL102 CPS recorded at 600 MHz and 318 K: (A) 1D ^{1}H and (B) 1D ^{1}H DOSY. DOSY removes the signals from low molecular weight compounds such as HOD to show signals from the hexasaccharide RU; the anomeric and some diagnostic ring signals are labeled for residues A to F.

The presence of the hexasaccharide RU was corroborated by 1D ^{13}C NMR overlaid with ^{13}C-DEPT, which gave six anomeric and five methylene groups, two of which were deshielded and designated as linkage carbons. The C═O signal at 175.7 ppm was attributed to C6 of GlcA (data not shown).

An overlay of COSY/TOCSY (**Fig. S1**) and a series of 1D TOCSY and NOESY experiments allowed full assignments of the six spin systems and identified the residues as: α-Glc (A), α-Gal (B), β-Gal^{I} (C), β-Gal^{II} (D), β-GlcA (E), and β-Glc (F). All the proton/carbon crosspeaks in the HSQC-DEPT spectrum (**Fig. S2**) were identified from proton assignments aided by HMBC long range ^{1}H/^{13}C intra-residue correlations and supported by HSQC-hybrid experiments (HSQC-TOCSY and HSQC-NOESY, data not shown). The chemical shift data and carbon glycosylation shifts are collected in **Table S2**. HMBC gave diagnostic intra-residue correlations from H5 and H4 of residue E to the folded COOH signal, confirming residue E as β-GlcA. The overlay with HSQC/HMBC of the anomeric region (Fig. 2) gave major intra-residue correlations: H1 to C3 and C5 for α-Glc (A) and α-Gal (B). The key inter-residue correlations of H1 of α-Glc (A) to C4 of β-GlcA (E), H1 of α-Gal (B) to C6 of β-Gal^{II} (D), H1 of β-Gal^{I} (C) to C4 of α-Gal (B), H1 of β-Gal^{II} (D) to C3 of β-Gal^{I} (C), H1 of β-GlcA (E) to C3 of α-Gal (B), and H1 of β-Glc (F) to C6 of α-Gal (B), establish the linkage positions and sequence of K102 as:

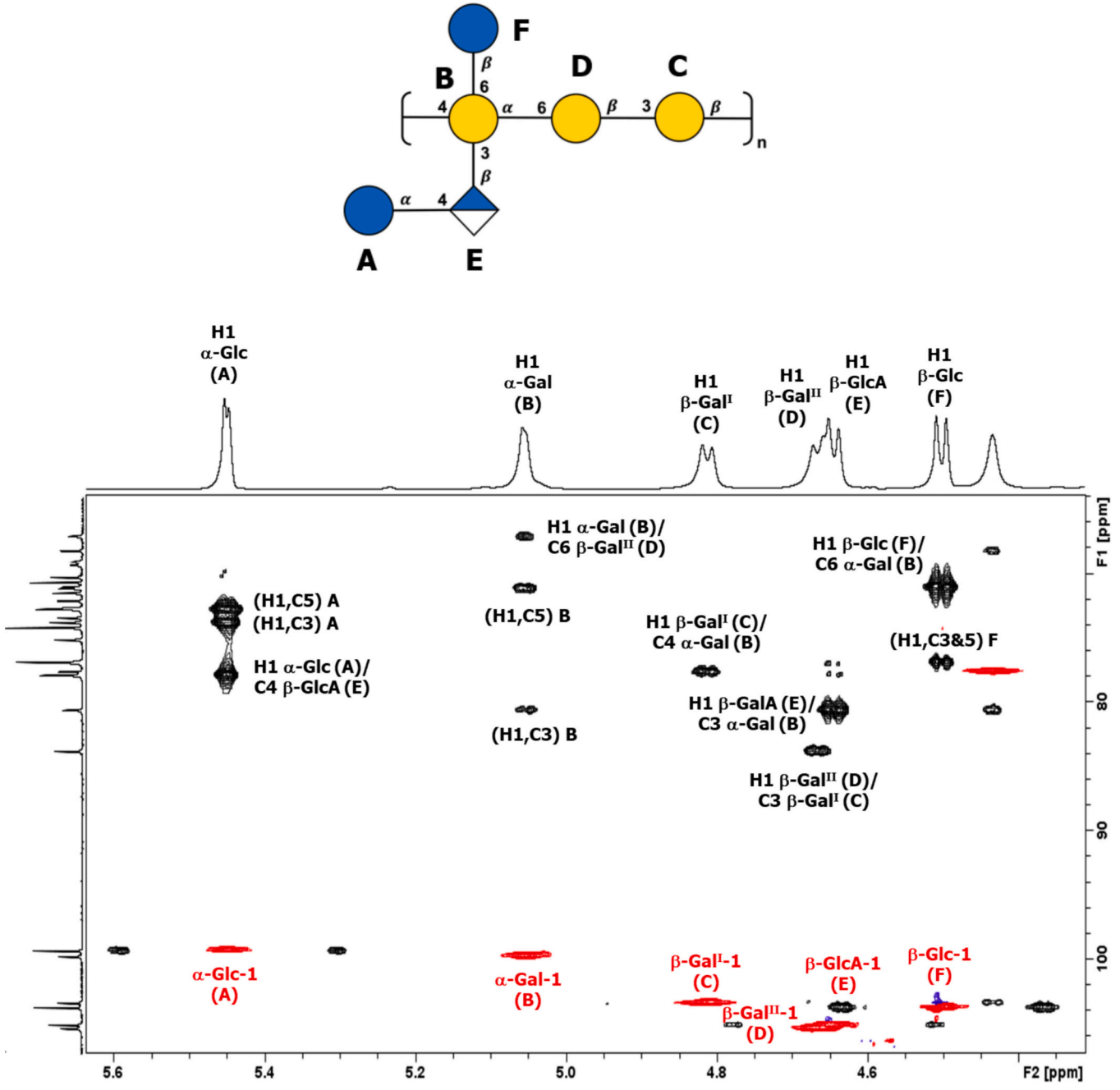

Fig. 2. ^{1}H—^{13}C NMR HSQC (red)/HMBC (black) overlay of the anomeric region of KL102 CPS recorded at 600 MHz and 318 K. The intra- and inter-residue proton/carbon crosspeaks for the hexasaccharide RU are labeled (A = α-Glc, B = α-Gal, C = β-Gal^{I}, D = β-Gal^{II}, E = β-GlcA, and F = β-Glc).

3.2. Structural determination of K112 CPS

A panel of *Kp* isolates obtained from Pakistan, India and Ethiopia and identified as potential new serotype KL112 was selected from the BARNARDS study (**Table S3** (Nonne et al., 2025)). The CPS was extracted from all isolates and its amount and saccharide length were determined through a high-level characterization (**Table S3**). Sugar amount varied from 4 to 37.6 μg/OD and MW from 391 to 662 kDa. All CPS shared same sugar composition as determined by HPAEC-PAD. The ST15 19,679 strain from India (Nonne et al., 2025) was selected as representative of KL112 and used for in depth structural analysis.

To perform structural characterization, the CPS was purified from strain 19,679 grown on plates as previously described (Nonne et al., 2024) and gave <2 % protein and < 1 % DNA impurities. It showed an average MW of 530 kDa, reduced to 300 kDa after sonication. HPAEC-PAD analysis indicated the presence of Man, Gal, and GlcA. Composition analysis using methanolysis followed by trimethylsilylation derivatisation and GLC-MS analysis confirmed the presence of Man, Gal and GlcA in the molar ratio of 1.5:1.0:0.4, suggesting the presence of a tetra- or pentasaccharide RU. Linkage analysis of the neutral monosaccharides, performed by GLC-MS analysis of the partially methylated alditol acetates identified: terminal Man*p*, 3-Gal*p*, 2,3-Man*p* in the molar ratio of 0.9:1.0:0.7. The glycosidic linkage of GlcA to C3 of Gal in the side chain was determined by NMR analysis; this also accounts for the low recovery of 3-Gal*p* in linkage analysis. The D absolute configuration was established for all sugar residues.

Detailed 1D and 2D ^{1}H and ^{13}C NMR experiments were performed on the KL112 CPS sample. A comparison of the 1D proton NMR and DOSY spectra (Fig. 3) showed that KL112 contains five anomeric signals (designated A to E) at 5.38, 5.18, 4.71, 4.63, and 4.54 ppm, consistent with the presence of a pentasaccharide RU with two α- and three β-monosaccharides.

The presence of the pentasaccharide was corroborated by 1D ^{13}C NMR overlaid with ^{13}C-DEPT, which gave five anomeric and four methylene groups. The C═O signal at 175.9 ppm was attributed to C6 of GlcA (data not shown).

An overlay of COSY/TOCSY (**Fig. S3**) and a series of 1D TOCSY and NOESY experiments allowed full assignments of the five spin systems and identified the residues as: α-Gal (A), α-Man (B), β-GlcA (C), β-Man (D), and β-Gal (E). All the proton/carbon crosspeaks in the HSQC-DEPT spectrum (**Fig. S4**) were identified from proton assignments aided by HMBC long range ^{1}H/^{13}C intra-residue correlations and HSQC-hybrid experiments (data not shown). The chemical shift data and carbon glycosylation shifts are collected in **Table S4**. HMBC gave diagnostic intra-residue correlations from H5 and H4 of residue C to the folded COOH signal, confirming residue C as β-GlcA. The overlay with HSQC/HMBC of the anomeric region (Fig. 4) gave intra-residue correlations: H1 to C3 and C5 for α-Gal (A), H1 to C2, C3 and C5 for α-Man (B) and H1 to C2 and C5 for β-Man (D). The key inter-residue correlations of H1 of α-Gal (A) to C3 of α-Man (B), H1 of α-Man (B) to C3 of β-Gal (E), H1 of β-GlcA (C) to C3 of α-Gal (A), H1 of β-Man (D) to C4 of β-GlcA (C), and H1 of β-Gal (E) to C2 of α-Man (B), establish the linkage positions and sequence of K112 as:

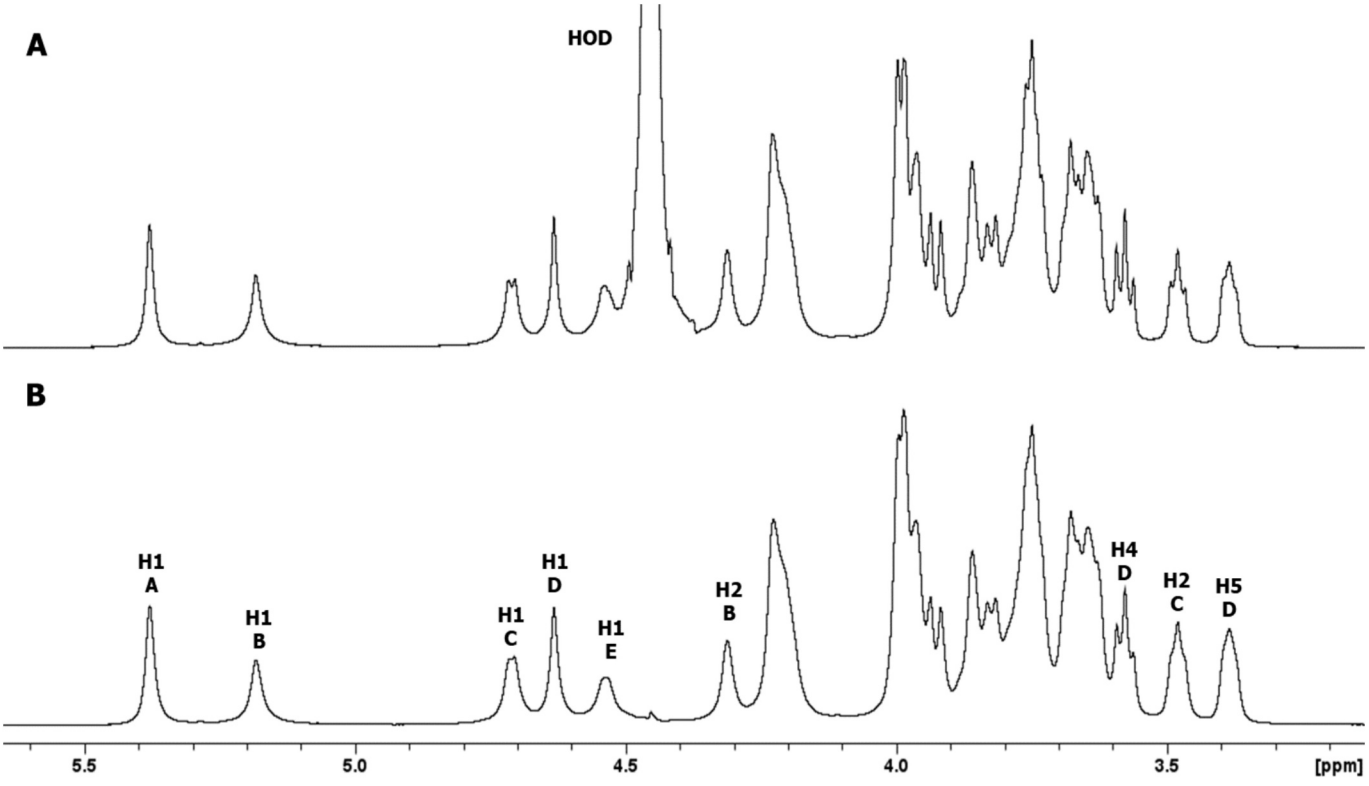

Fig. 3. ^{1}H NMR spectra of KL112 CPS recorded at 600 MHz and 333 K: (A) 1D ^{1}H and (B) 1D ^{1}H DOSY. DOSY removes the signals from low molecular weight compounds such as HOD to show signals from the pentasaccharide RU; the anomeric and some diagnostic ring signals are labeled for residues A to E.

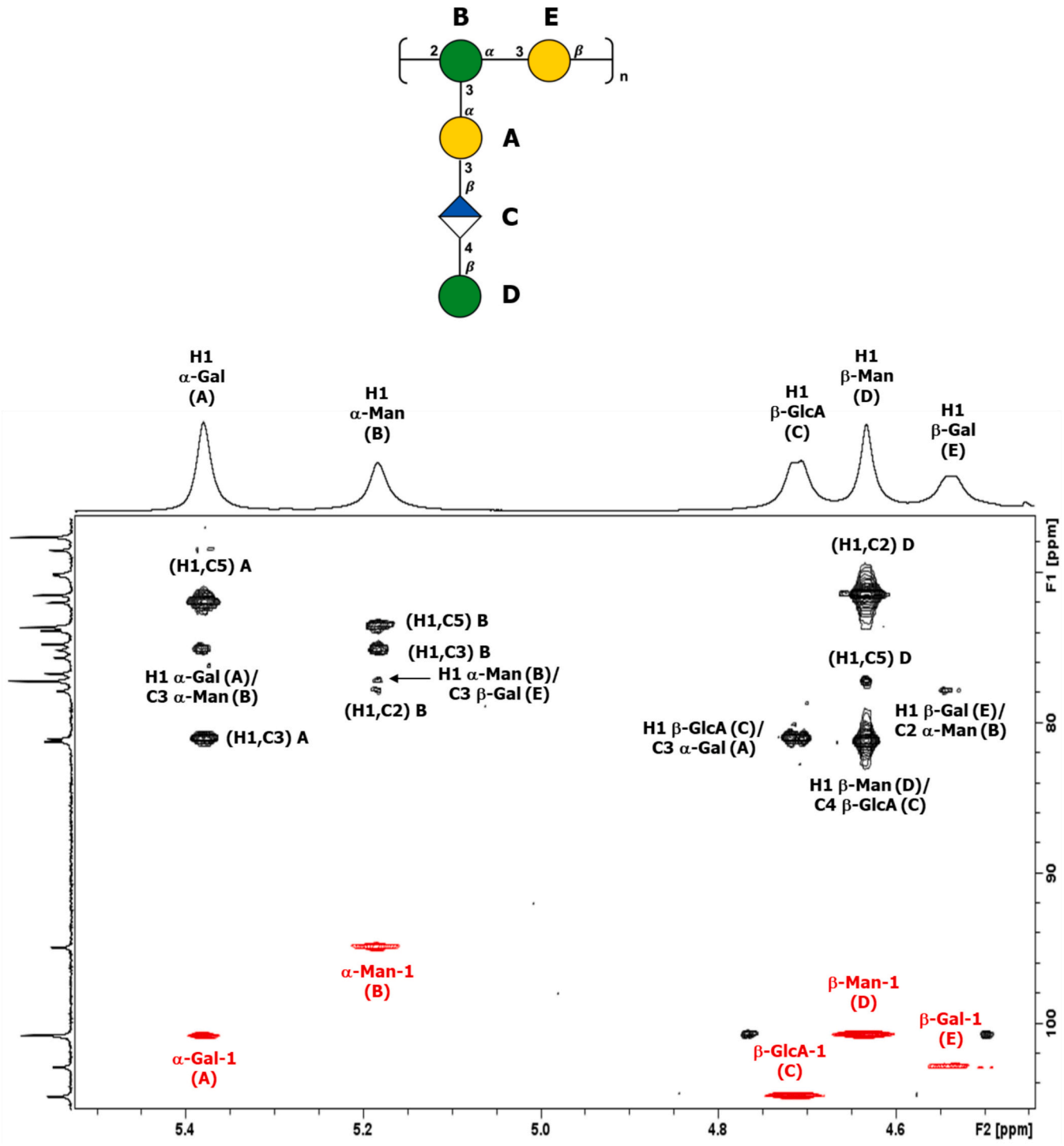

Fig. 4. $^{1}H—^{13}C$ NMR HSQC (red)/HMBC (black) overlay of the anomeric region of KL112 CPS recorded at 600 MHz and 333 K. The intra- and inter-residue proton/carbon crosspeaks for the pentasaccharide RU are labeled (A = α-Gal, B = α-Man, C = β-GlcA, D = β-Man, and E = β-Gal).

3.3. Investigating binding and functionality of K102 and K112 specific sera against a panel of homologous isolates from LMICs

K102 and K112 purified CPS reduced in size by sonication to approximately 109 and 294 KDa were chemically conjugated to CRM_{197} carrier protein following random activation using CDAP chemistry (Nappini et al., 2024). Resulting conjugates were characterized by a saccharide to protein ratio of 0.87 and 0.62 respectively, with no presence of free protein and free saccharide as detected by High Performance Liquid Chromatography–Size Exclusion Chromatography (HPLC-SEC). Rabbits were injected with K102 or K112 conjugates and the resulting polyclonal pooled sera, after having verified presence of CPS specific antibodies by ELISA, were tested for their ability to bind and kill the panel of homologous strains collected in the BARNARDS study (**Tables S1** and **S3**).

For K102 strains, analysis by flow cytometry (FC) showed sera binding to all isolates, that translated into serum bactericidal activity (Fig. 5A). For K112 strains instead, binding was verified for all isolates, except for 4 of the 18 strains (Fig. 5B), that displayed very low/no CPS on their surface (**Table S3**). Furthermore, binding of antibodies did not

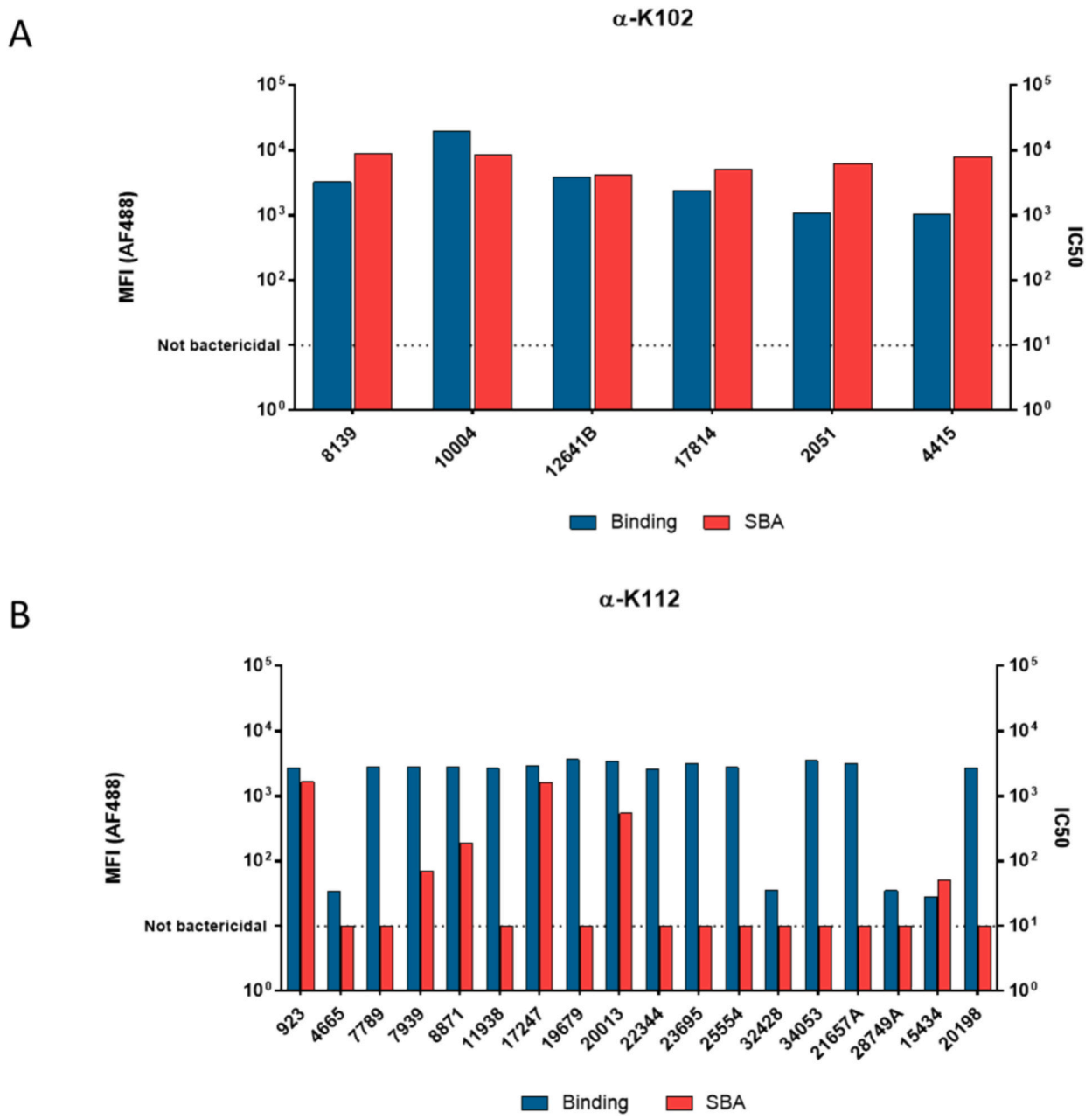

Fig. 5. Binding by flow cytometry and SBA titers of K102 (A) and K112 (B) polyclonal rabbit sera against a panel of homologous clinical isolates. "Not bactericidal" lines correspond to the titer assigned to pre-immune sera used as negative control. The test panels shown are single-run qualitative screens.

translate into sera functionality for all the isolates: 9 *Kp* that gave binding were not killed in SBA (Fig. 5B). Resistance to killing for K112 strains does not seem to be associated to the amount of CPS or its length.

3.4. Investigating cross-binding and cross-functionality of K102 and K112 specific sera against a panel of heterologous isolates from LMICs

Polyclonal sera specific to K102 and K112 were then tested against a large panel of isolates from the BARNARDS study sharing a diversity of K-types. Among all K-types tested (K2, K5, K15, K18, K24, K25, K28, K30, K34, K39, K62, K64, K102, KL105, K112, and KL128), available from our collection, certain cross-reactivity were observed and are summarized in Fig. 6.

For K102 cross-binding was identified by FC against K15, K18, K25, K34, KL105 and K112 strains. Cross-binding translated in cross-bactericidal activity for K-types K15 (16/23) and K112 only (2/18) (Fig. 6A). For K112, cross-binding was identified by FC against K18, K39, K102 and KL105 strains. Cross-binding translated into cross-bactericidal activity for K-types K39 (3/11) and KL105 (1/1) (Fig. 6B).

4. Discussion

Klebsiella pneumoniae is a major cause of nosocomial infections and neonatal sepsis worldwide (Dangor et al., 2024). Given the rise of antimicrobial resistance, the World Health Organization has included this pathogen among those for which the development of new interventions is a global health priority.

Capsular polysaccharides have been proposed as protective targets for a vaccine against *Kp* (Arato, Raso, Gasperini, Berlanda Scorza, & Micoli, 2021). The strong association of few K-types to high-risk *Kp* clones, which experienced a global diffusion and are the major cause of severe infections at a global scale, strongly reinforce this idea.

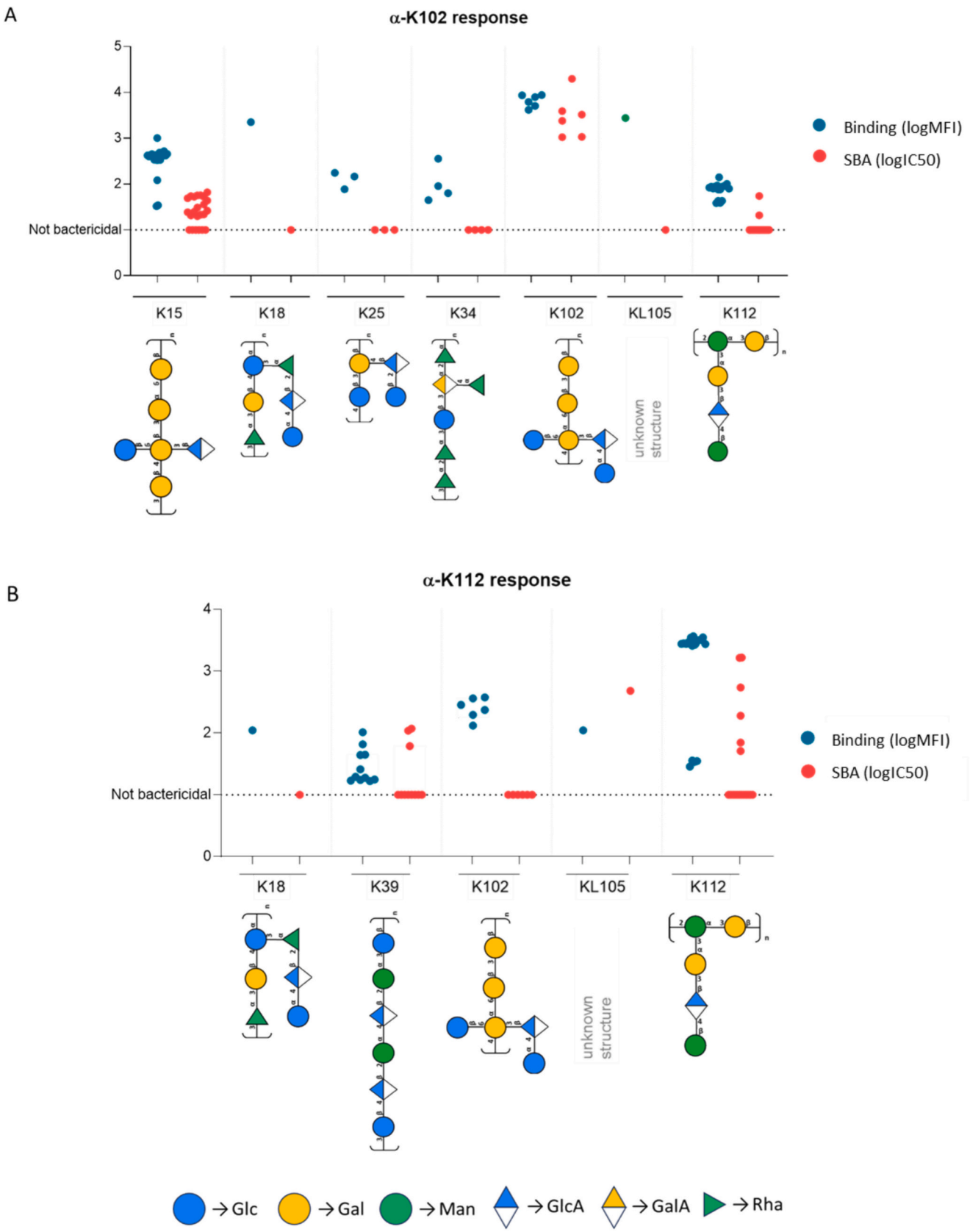

Fig. 6. Binding by flow cytometry and SBA titers of K102 (A) and K112 (B) polyclonal rabbit sera against a panel of heterologous clinical isolates (each dot represents result for an individual strain) for which cross-reactivity was observed. The test panels shown are single-run qualitative screens.

Historically, *Kp* has been classified based on capsule typing by serological methods, even if these has been gradually substituted by several genotyping schemes in the last years. The latter approach revealed that some genotypes are linked to CPS which have not been chemically determined yet. Structural characterization is critical for the design of a vaccine and serves as the basis for selecting the most appropriate technology for CPS presentation while preserving its structural integrity. It also helps to understand which epitopes are critical for immune responses and protection, and the development of appropriate analytical methods for antigen quantification and monitoring vaccine stability over time. Furthermore, similarity with CPS structures already known that share common epitopes could result in simplification of the final vaccine formulation.

Here we have resolved the structure of two novel most prevalent K-genotypes: KL102, which has been previously linked to *Kp* strains of ST307, and KL112, strongly associated to the major clade of the *Kp* ST15 high-risk clone. K102 is the first *Kp* serotype reported to have a 3 + 2 + 1 type hexasaccharide repeating unit; the presence of a hexose-uronic acid in the side chain has also been reported for serotypes K12 (Dutton & Savage, 1980), K18 (Dutton, Savage, & Vignon, 1980), K28 (Curvall, Lindberg, & Lönngren, 1975), K36 (Dutton & Mackie, 1977), K41 (Joseleau, Lapeyre, Vignon, & Dutton, 1978), KK207–2(Bellich et al., 2019) and K112 (this study). Likewise, K112 also has a novel structure as it is the first *Kp* serotype reported to have a 2 + 3 type pentasaccharide repeating unit. KK207–2 has an unusual 2 + 4 type hexasaccharide repeating unit and there are several serotypes with a 2 + 2 type tetrasaccharide repeating unit including K20, which interestingly has the identical structure as K112 but without the terminal β-Man residue on the side chain (Choy & Dutton, 1973). Structural determination is also key to confirm genomic prediction and support epidemiology studies to look at global prevalence of the different serotypes, helping to define an optimal vaccine composition for a good coverage.

Here, importantly we have demonstrated that these two novel CPS, K102 and K112, conjugated to a carrier protein, can generate a good immune response in animals, with antibodies able to bind and kill in vitro a panel of homologous clinical isolates.

Cross-binding with heterologous serotypes measured by FC shows that the antibodies raised by vaccination with the chosen antigen recognize and bind to similar structural features/epitopes presented by the non-vaccine serotype. This antibody binding could result in functional activity or not, which can be measured through neutralization, opsonophagocytosis, or as in this case bactericidal assays. If functional, then cross-protection against disease caused by the second serotype may be possible through the cross-reactive antibodies elicited by the vaccine. This is important for the development of multivalent vaccines against disease caused by many different serotypes of *Kp*, as cross-protection allows for reduction of the vaccine components and results in significant cost reduction for a vaccine targeting neonatal sepsis in LMICs.

The structural basis of cross-protection is a topic for ongoing investigation. Studies published on the surface carbohydrate antigens of *Shigella flexneri*, pneumococcal and meningococcal bacteria show that cross-protection relies on the presence of common conformational and structural epitopes, and that side chain residues, accessible for binding, are important (Feemster et al., 2024; Gómez-Redondo, Ardá, Gimeno, & Jiménez-Barbero, 2020; Haji-Ghassemi, Blackler, Martin Young, & Evans, 2015; Richardson, Kuttel, & Ravenscroft, 2022). Further, the presence of carboxyl or methyl groups on the carbohydrate repeating unit structure can lead to higher affinities by permitting additional ionic or hydrophobic interactions (Haji-Ghassemi et al., 2015).

For the serotype K102 vaccine, the strongest bactericidal cross-reactivity was against K15 which also has a Gal backbone and β-GlcA in the side chain, whereas the weaker cross-reactivity against K112 could arise from β-GlcA present in the side chain trisaccharide. For the serotype K112 vaccine, the strongest bactericidal cross-reactivity was against K39 which has a Man-β-GlcA disaccharide present in the backbone also present in the K112 side chain; the RU structure of serotype K105 is unknown. The cross-reactivity observed could be due to low level (<2 %) of impurities (e.g. proteins and OAg) detected in purified CPS used to generate hyperimmune sera and in this study we did not perform experiments after sera adsorption to exclude this possibility. However, the functional activity elicited against heterologous strains was limited, suggesting that incorporating the prevalent emerging serotypes K102 and K112 into a vaccine is unlikely to offer significant protection against heterologous K-types (Sands et al., 2021).

Overall, our work on the structural elucidation of two CPS structures prevalent in two major *Kp* high-risk clones, the development of K102 and K112 glycoconjugates and cross-reactivity studies constitute an important contribution towards the development of a saccharide-based vaccine against *Kp* infections.

CRediT authorship contribution statement

Neil Ravenscroft: Writing – review & editing, Writing – original draft, Supervision, Methodology, Formal analysis, Conceptualization. **Francesca Nonne:** Writing – review & editing, Methodology, Investigation, Formal analysis. **Gianina Florentina Belciug:** Writing – review & editing, Methodology, Investigation, Formal analysis. **Michela Zaro:** Writing – review & editing, Methodology, Investigation, Formal analysis. **Mariagrazia Molfetta:** Writing – review & editing, Methodology, Investigation, Formal analysis. **Roberta Di Benedetto:** Writing – review & editing, Methodology, Investigation, Formal analysis. **Renzo Alfini:** Writing – review & editing, Methodology, Investigation, Formal analysis. **Siwaphiwe Mfana:** Writing – review & editing, Methodology, Investigation, Formal analysis. **Barbara Bellich:** Writing – review & editing, Methodology, Investigation, Formal analysis. **Marco Maria D'Andrea:** Writing – review & editing, Supervision, Methodology, Formal analysis, Conceptualization. **Martina Carducci:** Writing – review & editing, Supervision, Methodology, Formal analysis, Conceptualization. **Omar Rossi:** Writing – review & editing, Supervision, Methodology, Formal analysis, Conceptualization. **Carlo Giannelli:** Writing – review & editing, Writing – original draft, Supervision, Methodology, Formal analysis, Conceptualization. **Paola Cescutti:** Writing – review & editing, Writing – original draft, Supervision, Methodology, Formal analysis, Conceptualization. **Francesca Micoli:** Writing – original draft, Supervision, Methodology, Funding acquisition, Formal analysis, Conceptualization.

Declaration of competing interest

The authors declare the following financial interests/personal relationships which may be considered as potential competing interests: Francesca Micoli reports financial support was provided by Gates Foundation. This work was performed at the request of and sponsored by GlaxoSmithKline Biologicals SA. GSK Vaccines Institute for Global Health SRL is an affiliate of GlaxoSmithKline Biologicals SA. Gianina Florentina Belciug, Mariagrazia Molfetta, Roberta Di Benedetto, Renzo Alfini, Martina Carducci, Omar Rossi, Carlo Giannelli, and Francesca Micoli are employees of the GSK group of companies. Francesca Nonne was employee of the GSK group of companies when the study was performed. Francesca Micoli, Carlo Giannelli and Omar Rossi report ownership of GSK shares.

Acknowledgments

Authors thank the BARNARDS study team who collected and sequenced the isolates, in particular the lead investigators Tim Walsh, Kirsty Sands, Kenneth Iregbu, Rabaab Zahra, Grace Chan, Sulagna Basu, and Jean-Baptiste Mazarati; Nadia Boisen and Flemming Scheutz from the Statens Serum Institut for providing sharing copies of the isolates for this study. When the experiments were performed Barbara Bellich was working at the University of Trieste, Department of Life Sciences, Via L. Giorgieri 1, Trieste, Italy. This project was partially funded by a grant

from the Gates Foundation (grant number INV-033019).

Appendix A. Supplementary data

Supplementary data to this article can be found online at https://doi.org/10.1016/j.carbpol.2025.124385.

Data availability

Data will be made available on request.

References

Albersheim, P., Nevins, D. J., English, P. D., & Karr, A. (1967). A method for the analysis of sugars in plant cell-wall polysaccharides by gas-liquid chromatography. *Carbohydrate Research, 5*(3), 340–345.

Arato, V., Raso, M. M., Gasperini, G., Berlanda Scorza, F., & Micoli, F. (2021). Prophylaxis and Treatment against Klebsiella pneumoniae: Current Insights on This Emerging Anti-Microbial Resistant Global Threat. *International Journal of Molecular Sciences, 22*(8).

Argimón, S., David, S., Underwood, A., Abrudan, M., Wheeler, N. E., Kekre, M., & Aanensen, D. M. (2021). Rapid Genomic Characterization and Global Surveillance of Klebsiella Using Pathogenwatch. *Clinical Infectious Diseases, 73*(Suppl_4), S325–s335.

Bellich, B., Ravenscroft, N., Rizzo, R., Lagatolla, C., D'Andrea, M. M., Rossolini, G. M., & Cescutti, P. (2019). Structure of the capsular polysaccharide of the KPC-2-producing Klebsiella pneumoniae strain KK207-2 and assignment of the glycosyltransferases functions. *International Journal of Biological Macromolecules, 130*, 536–544.

Cejas, D., Magariños, F., Elena, A., Ferrara, M., Ormazábal, C., Yernazian, M. V., & Radice, M. (2022). Emergence and clonal expansion of Klebsiella pneumoniae ST307, simultaneously producing KPC-3 and NDM-1. *Revista Argentina de Microbiología, 54*(4), 288–292.

Choy, Y.-M., & Dutton, G. G. S. (1973). Structure of the Capsular Polysaccharide of Klebsiella K-type 20. *Canadian Journal of Chemistry, 51*(18), 3015–3020.

Curvall, M., Lindberg, B., & Lönngren, J. (1975). Structural studies of the capsular polysaccharide of *Klebsiella* type 28. *Carbohydrate Research, 42*(1), 95–105.

Dangor, Z., Benson, N., Berkley, J. A., Bielicki, J., Bijsma, M. W., Broad, J., & Madhi, S. A. (2024). Vaccine value profile for Klebsiella pneumoniae. *Vaccine, 42*(19s1), S125–s141.

Dutton, G. G., & Mackie, K. L. (1977). Structural investigation of *Klebsiella* serotype K36 polysaccharide. *Carbohydrate Research, 55*, 49–63.

Dutton, G. G. S., & Savage, A. V. (1980). Structural investigation of the capsular polysaccharide of *Klebsiella* serotype K12. *Carbohydrate Research, 83*(2), 351–362.

Dutton, G. G. S., Savage, A. V., & Vignon, M. (1980). Use of a bacteriophage to depolymerize a polysaccharide to an oligosaccharide; comparison of the 1H and 13C nuclear magnetic resonance spectra of the polymer and its hexasaccharide repeating unit. *Canadian Journal of Chemistry, 58*(23), 2588–2591.

Feemster, K., Hausdorff, W. P., Banniettis, N., Platt, H., Velentgas, P., Esteves-Jaramillo, A., & Buchwald, U. K. (2024). Implications of cross-reactivity and cross-protection for pneumococcal vaccine development. *Vaccines, 12*(9) (Basel).

Feng, L., Zhang, M., & Fan, Z. (2023). Population genomic analysis of clinical ST15 *Klebsiella pneumoniae* strains in China. *Frontiers in Microbiology, 14*, Article 1272173.

Gerwig, G. J., Kamerling, J. P., & Vliegenthart, J. F. G. (1979). Determination of the absolute configuration of mono-saccharides in complex carbohydrates by capillary G.L.C. *Carbohydrate Research, 77*, 10–17.

Gerwig, G. J., Kamerling, J. P., & Vliegenthart, J. F. G. (1978). Determination of the d and l configuration of neutral monosaccharides by high-resolution capillary g.l.c. *Carbohydrate Research, 62*(2), 349–357.

Global burden of bacterial antimicrobial resistance in 2019. (2022). a systematic analysis. *The Lancet, 399*(10325), 629–655.

Gómez-Redondo, M., Ardá, A., Gimeno, A., & Jiménez-Barbero, J. (2020). Bacterial polysaccharides: conformation, dynamics and molecular recognition by antibodies. *Drug Discovery Today: Technologies, 35-36*, 1–11.

Gonzalez-Ferrer, S., Peñaloza, H. F., Budnick, J. A., Bain, W. G., Nordstrom, H. R., Lee, J. S., & Van Tyne, D. (2021). Finding Order in the Chaos: Outstanding Questions in Klebsiella pneumoniae Pathogenesis. *Infection and Immunity, 89*(4).

Haji-Ghassemi, O., Blackler, R. J., Martin Young, N., & Evans, S. V. (2015). Antibody recognition of carbohydrate epitopes†. *Glycobiology, 25*(9), 920–952.

Hall, G. S. (2013). Bailey & Scott's Diagnostic Microbiology, 13th Edn. *Laboratory Medicine, 44*(4), e138–e139.

Harris, P. J., Henry, R. J., Blakeney, A. B., & Stone, B. A. (1984). An improved procedure for the methylation analysis of oligosaccharides and polysaccharides. *Carbohydrate Research, 127*(1), 59–73.

Joseleau, J.-P., Lapeyre, M., Vignon, M., & Dutton, G. G. S. (1978). Chemical and n.m.r.-spectroscopic investigation of the capsular polysaccharide of klebsiella serotype k41. *Carbohydrate Research, 67*(1), 197–212.

Kakehi, K., & Honda, S. (2021). Silyl Ethers of Carbohydrates. In *Analysis of Carbohydrates by GLC and MS* (pp. 43–85).

Kumar, C. K., Sands, K., Walsh, T. R., O'Brien, S., Sharland, M., Lewnard, J. A., & Laxminarayan, R. (2023). Global, regional, and national estimates of the impact of a maternal *Klebsiella pneumoniae* vaccine: A bayesian modeling analysis. *PLoS Medicine, 20*(5), Article e1004239.

Lam, M. M. C., Wick, R. R., Judd, L. M., Holt, K. E., & Wyres, K. L. (2022). Kaptive 2.0: Updated capsule and lipopolysaccharide locus typing for the *Klebsiella pneumoniae* species complex. *Microbial Genomics, 8*(3).

Lundborg, M., & Widmalm, G. (2011). Structural analysis of glycans by NMR chemical shift prediction. *Analytical Chemistry, 83*(5), 1514–1517.

Mandell, Douglas, & Bennett's Principles and Practice of Infectious Diseases (Eighth Edition). (2015). *Philadelphia*. W.B. Saunders.

Nappini, R., Alfini, R., Durante, S., Salvini, L., Raso, M. M., Palmieri, E., & Giannelli, C. (2024). Modeling 1-Cyano-4-dimethylaminopyridine Tetrafluoroborate (CDAP) Chemistry to Design Glycoconjugate Vaccines with Desired Structural and Immunological Characteristics. *Vaccines (Basel), 12*(7), 707.

Necchi, F., Saul, A., & Rondini, S. (2017). Development of a high-throughput method to evaluate serum bactericidal activity using bacterial ATP measurement as survival readout. *PLoS One, 12*(2), Article e0172163.

Nonne, F., Molfetta, M., Belciug, G. F., Carducci, M., Cianchi, V., Zakroff, C., & Micoli, F. (2025). The characterization of *Klebsiella pneumoniae* associated with neonatal sepsis in low- and middle-income countries to inform vaccine design. *Communications Biology, 8*(1), 898.

Nonne, F., Molfetta, M., Nappini, R., La Guidara, C., Di Benedetto, R., Mfana, S., … Giannelli, C. (2024). Development and application of a high-throughput method for the purification and analysis of surface carbohydrates from *Klebsiella pneumoniae*. *Biology, 13*(4) (Basel).

Opoku-Temeng, C., Malachowa, N., Kobayashi, S. D., & DeLeo, F. R. (2022). Innate Host Defense against Klebsiella pneumoniae and the Outlook for Development of Immunotherapies. *Journal of Innate Immunity, 14*(3), 167–181.

Peirano, G., Chen, L., Kreiswirth, B. N., & Pitout, J. D. D. (2020). Emerging Antimicrobial-Resistant High-Risk Klebsiella pneumoniae Clones ST307 and ST147. *Antimicrobial Agents and Chemotherapy, 64*(10).

Richardson, N. I., Kuttel, M. M., & Ravenscroft, N. (2022). Modeling of pneumococcal serogroup 10 capsular polysaccharide molecular conformations provides insight into epitopes and observed cross-reactivity. *Frontiers in Molecular Biosciences, 9*, Article 961532.

Rodrigues, C., Lanza, V. F., Peixe, L., Coque, T. M., & Novais, Â. (2023). Phylogenomics of globally spread clonal groups 14 and 15 of *Klebsiella pneumoniae*. *Microbiology Spectrum, 11*(3), Article e0339522.

Rossi, O., Molesti, E., Saul, A., Giannelli, C., Micoli, F., & Necchi, F. (2020). Intra-Laboratory Evaluation of Luminescence Based High-Throughput Serum Bactericidal Assay (L-SBA) to Determine Bactericidal Activity of Human Sera against Shigella. *High Throughput, 9*(2).

Sands, K., Carvalho, M. J., Portal, E., Thomson, K., Dyer, C., Akpulu, C., & Walsh, T. R. (2021). Characterization of antimicrobial-resistant Gram-negative bacteria that cause neonatal sepsis in seven low- and middle-income countries. *Nature Microbiology, 6*(4), 512–523.

Stanton, T. D., Hetland, M. A. K., Löhr, I. H., Holt, K. E., & Wyres, K. L. (2025). Fast and accurate *in silico* antigen typing with Kaptive 3. *Microbial Genomics, 11*(6), Article 001428.

Sweet, D. P., Shapiro, R. H., & Albersheim, P. (1975). Quantitative analysis by various g. l.c. response-factor theories for partially methylated and partially ethylated alditol acetates. *Carbohydrate Research, 40*(2), 217–225.

WHO bacterial priority pathogens list. (). *Bacterial pathogens of public health importance to guide research, development and strategies to prevent and control antimicrobial resistance. 2024*.

Wyres, K. L., Nguyen, T. N. T., Lam, M. M. C., Judd, L. M., van Vinh Chau, N., Dance, D. A. B., & Holt, K. E. (2020). Genomic surveillance for hypervirulence and multi-drug resistance in invasive Klebsiella pneumoniae from South and Southeast Asia. *Genome Medicine, 12*(1), 11.

Wyres, K. L., Wick, R. R., Gorrie, C., Jenney, A., Follador, R., Thomson, N. R., & Holt, K. E. (2016). Identification of *Klebsiella* capsule synthesis loci from whole genome data. *Microbial Genomics, 2*(12), Article e000102.

Xu, L., Jiayang, L., Wenqi, W., Xiuwen, W., & Ren, J. (2024). *Klebsiella pneumoniae* capsular polysaccharide: Mechanism in regulation of synthesis, virulence, and pathogenicity. *Virulence, 15*(1), 2439509.